Taguchi-Based Optimization of Mix Design and Mechanical Properties of Epoxy Polymer Concrete with Recycled Coarse Aggregate

Khusnul Aldi Saputra*
Department of Civil Engineering
Universitas Brawijaya
Malang, Indonesia
khusnulaldisaputra@gmail.com

Eva Arifi
Department of Civil Engineering
Universitas Brawijaya
Malang, Indonesia
evaarifi@ub.ac.id

Desy Setyowulan
Department of Civil Engineering
Universitas Brawijaya
Malang, Indonesia
desy_wulan@ub.ac.id

Abstract*—This study examines the mix design and mechanical properties of epoxy polymer concrete utilizing fully recycled coarse aggregate and fly ash as a mineral filler through a Taguchi-based optimization framework. An L9 orthogonal array including four control factors and three levels was employed to incorporate epoxy resin content, resin–hardener ratio, coarse-to-fine aggregate ratio, and class C fly ash proportion. All mixtures were designed using the absolute-volume method so that the total volume of the constituent materials exactly matched the target specimen volume. The research test object was a 50 × 50 × 50 mm cube that follows the experimental design in method B of the ASTM C 579-96 standard for polymer concrete. Cube specimens tested at seven days for compressive strength and static modulus of elasticity based on the stress–strain response. The compressive strengths varied from around 11.14 to 57.20 MPa, whereas the average static modulus ranged from about 0.58 GPa to nearly 2.95 GPa. Taguchi analysis and ANOVAs conducted on both mean strength and S/N ratios consistently revealed epoxy content, resin–hardener ratio, and coarse-to-fine aggregate ratio as the dominant factors, while fly ash served as a secondary modifier. The optimal combination comprises 25% polymer matrix of the total specimen volume, a resin–hardener ratio of 1.5:1, a balanced coarse-to-fine aggregate ratio of 1:1, and an quantity of fly ash around 30% of the total volume of fine aggregate. According to Taguchi analysis, this optimal combination leads to a predicted compressive strength of approximately 52.89 to 61.23 MPa. An independent confirmation mixture prepared at this optimal combination achieved an average strength of about 57.46 MPa, aligning well with Taguchi predictions. The linear relationship between compressive strength and static modulus of elasticity shows a positive correlation. This linear relationship enables a straightforward empirical formula to determine the stiffness of epoxy polymer concrete with recycled coarse material, predicated on its compressive strength.

Keywords—Compressive Strength, Modulus of Elasticity, Polymer Concrete, Recycled Aggregate, Taguchi Method

I. INTRODUCTION

High-performance and sustainable construction materials are a priority due to the limitations of ordinary Portland cement (OPC) concrete, including vulnerability in harsh environments and high CO_2 footprint of clinker production [1]–[4]. Polymer concrete (PC), which employs a thermoset resin to partially or wholly substitute the cementitious binder, has been found to be an effective alternative due to its high compressive and flexural strength, minimal permeability, rapid strength development, and exceptional chemical resistance [4]–[6]. These characteristics result from a thick, cross-linked polymer matrix that efficiently adheres mineral aggregates and restricts the movement of fluids and aggressive ions [3], [6]. However, the design principles for PC remain less advanced than those for OPC. The mix design process often relies on empirical knowledge, especially for epoxy-based systems used in structural applications [3], [4].

The macroscopic performance of polymer concrete is governed to a large extent by its internal microstructure, especially resin volume fraction, aggregate packing, and porosity [3], [4], [6]. Ferdous *et al.* showed that both the resin-to-filler ratio and the matrix-to-aggregate ratio exert a decisive influence on strength and durability [4]. Smoleń *et al.* systematically varied polyester resin volume fraction between 5–30% and reported that increasing resin content generally enhances apparent density and mechanical properties while reducing open porosity and water absorption, although excessive resin for large-size aggregates leads to reduced flexural strength and inefficient material usage [3]. These studies underline that there exists an optimum range of resin volume fraction where the resin not only acts as a binder but also contributes significantly to load transfer, while outside this range the presence of microvoids, resin-rich zones, or shrinkage-induced defects can degrade mechanical performance [3], [4], [6].

For epoxy systems, the chemistry of the binder further complicates mix design. The stoichiometric balance between epoxy equivalent weight and active hydrogen equivalent weight of the curing agent controls cross-link density, glass transition temperature, stiffness, and fracture behavior [4], [7]. Deviations from stoichiometry lead to unreacted epoxy or amine groups that behave as internal plasticizers, lowering modulus and strength and increasing long-term deformation under load [4], [7]. According to Ferdous *et al.*, a minimum filler concentration of approximately 40% is required to mitigate severe coarse aggregate segregation, thereby optimizing network uniformity and improving mechanical properties [4]. Consequently, resin volume fraction, resin–hardener stoichiometry, and aggregate skeleton must be considered together when seeking an optimal epoxy polymer concrete mix [6].

The construction sector under significant pressure to diminish the use of natural aggregates and construction and demolition waste, in accordance with circular economy plans [5], [8]. Comprehensive reviews indicate that recycled coarse aggregate (RCA) from crushed concrete can significantly mitigate environmental impacts; however, it often results in increased porosity, enhanced water absorption, and microcracking associated with adhered old mortar [8]–[10]. Kępniak *et al.* showed that in the case of polymer concrete, replacing full natural aggregate with full recycled aggregate

 EISSN: 2961-872X ●PISSN: 2961-8924●DOI: 10.56741/IISTR.esl.002091

can actually make it stronger (from 89.1 MPa to 96 MPa) because a double-layer shell of resin and calcium-based microfiller forms around the porous recycled grains [5]. This is only true if the right resin system and aggregate gradation are chosen [5]. These findings imply that 100% RCA can be a technically viable and environmentally desirable aggregate for epoxy polymer concrete provided resin content, RCA properties, and packing density are tuned [5], [8], [9].

The mix design of polymer concrete is inherently a multifactorial process, wherein the individual constituents interact non-linearly to govern the resulting concrete strength [3], [4], [6], [11]. The experimental design should comply with relevant standards such as ASTM C 579–96 or ACI 548.1R-09 for polymer concrete [12], [13]. Conducting a full-factorial experimental program to investigate all combinations would be excessively expensive for materials, time, and testing [14]–[16]. In these circumstances, the Taguchi method offers an effective quality-engineering framework for parameter design. The Taguchi method employs orthogonal arrays to analyze the combined effects of multiple control factors and utilizes signal-to-noise (S/N) ratios and mean value to identify robust settings that optimize performance while minimizing sensitivity to uncontrolled variability [14]–[16]. For characteristics characterized by "larger-is-better" the Taguchi method systematically converts response data into signal-to-noise (S/N) ratios, performs analysis of variance (ANOVA) on these ratios, and subsequently estimates the anticipated performance at the predicted optimal factor combination [14], [15]. Previous civil engineering applications have shown that the Taguchi method can greatly reduce the number of test RUNs while still giving statistically significant rankings of how important different factors are for concrete, mortars, and geotechnical materials [17]–[20].

Even though epoxy polymer concrete design and recycled aggregate use have improved [3]–[5], [7], [8], most previous studies have examined polymer concrete by focusing separately on resin type, resin volume fraction, filler content, or aggregate substitution. Limited attention has been given to the integrated optimization of epoxy polymer concrete containing 100% recycled agregate using a statistically structured mix-design approach. Therefore, this study addresses this gap by applying the Taguchi method and absolute-volume mix design to identify the dominant factors controlling compressive strength and static modulus of elasticity. The proposed approach advances theoretical understanding by clarifying the relative contribution of polymer matrix content, resin–hardener ratio, coarse-to-fine aggregate ratio, and fly ash content. Specifically, this study aims to identify the dominant mix-design factors through Taguchi method and ANOVA, determine the optimum mixture combination, and formulate data-driven recommendations for producing structurally efficient and environmentally sustainable epoxy polymer concrete containing 100% RCA.

II. Materials and Methods

A. Epoxy Resin and Curing Agent

The binder system comprised a commercial bisphenol-A liquid epoxy resin (Bakelite® EPR 174) and a cycloaliphatic amine hardener agent (Bakelite® EPH 555). EPR 174 and EPH 555 provided by PT Justus Kimiaraya, as shown in Fig. 1. The epoxy resin is an unmodified epichlorohydrin–bisphenol-A system demonstrating medium to high viscosity and a high heat-distortion temperature. The hardener agent is a low-viscosity cycloaliphatic amine. Table 1 presents the technical properties of the resin and hardener. The technical specifications were used to verify that the selected resin–hardener volume ratios closely adhered to stoichiometric balance and facilitated the systematic adjustment of cross-link density in the Taguchi design.

Table 1. Technical Properties of the Binder System

Properties	EPR 174	EPH 555
Viscosity at 25 °C	13.0 ± 2.0 MPa·s	0.5 – 1.0 poise
Epoxy Equivalent	189 ± 5 g/equiv.	-
Epoxy Value	0.53 equiv./100 g	-
Active Hydrogen Equivalent	-	86 g/equiv.
Amine Value	-	325 Mg KOH/g
Density at 25 °C	1.17 ± 0.01 g/cm³	1.010 g/cm³



Fig. 1. EPR 174 and EPH 555

B. Recycled Coarse Aggregate, Natural Fine Aggregate, and Fly Ash

The coarse aggregate used in all mixtures was 100% RCA produced by crushing discarded normal-strength concrete cylinders ($f_c' \geq 30$ MPa). As shown in Fig. 2, the RCA possessed a nominal maximum size of 10 mm. The RCA was only cleaned with running water and oven-dried prior to use, without any other pre-treatment, to accurately reflect practical recycling conditions. Fine aggregate using natural river sand that mostly passes sieve No. 8 (2.36 mm) is shown in Fig 2. Class C fly ash, compliant with ASTM C618, was utilized as a mineral filler and as a volumetric replacement for a portion of the fine aggregate [21]. In all mixtures, the volume of fly ash was specified as a percentage of the total fine aggregate volume, in accordance with the Taguchi factor specification. In all mixtures, the volume of fly ash was specified as a percentage of the total fine aggregate volume, in accordance with the Taguchi factor specification. Table 2 presents the outcomes of aggregate testing conducted in the laboratory and literature reviews on fly ash.



Fig. 2. Recycled Coarse Aggregate and Natural Fine Aggregate

C. Absolute-Volume Mix Design

All mixtures were designed using the absolute-volume method so that the total volume of resin, hardener, aggregates, and fly ash exactly matched the target specimen volume. For each mixture, the necessary volume V_i of component i was

derived from its specified volume fraction ϕ_i and the total specimen volume V_{tot}.

$$V_i = \phi_i V_{\text{tot}} \quad \text{with} \quad \sum_i \phi_i = 1 \tag{1}$$

The matching mass m_i was subsequently computed from the measured specific density ρ_i of each component.

$$m_i = \rho_i \, V_i \tag{2}$$

Four control factors were modified in the mix design [Table 3]. Factor A denotes the polymer matrix, represented as a percentage of the total specimen volume. Factor B denotes the volumetric ratio of resin to hardener utilized to partition the total binder volume into epoxy and curing-agent sub-fractions. Factor C is the coarse-to-fine aggregate volume ratio for each level the aggregate volumes were scaled so that

$$\phi_{\text{c}} : \phi_{\text{f,tot}} = \text{C}_1 : \text{C}_2 \tag{3}$$

where ϕ_{c} represents the RCA volume percentage and $\phi_{\text{f,tot}}$ denotes the total volume fraction of fine aggregate and fly ash. Factor D is the proportion of fly ash within the overall fine aggregate volume as described by

$$\phi_{\text{Fly Ash}} = \text{D}\% \; \phi_{\text{f,tot}} \tag{4}$$

$$\phi_{\text{Sand}} = \phi_{\text{f,tot}} - \phi_{\text{Fly Ash}} \tag{5}$$

For each mixture, the intended specimen volume V_{tot} was initially established. The binder volume was calculated based on factor A; the resin and hardener volumes were then obtained from factor B. The necessary volumes of RCA, natural sand, and fly ash were computed from factors C and D so that the sum of all volume fractions satisfied. Ultimately, all volumes were transformed into masses utilizing Eq. (2), and the batch weights were adjusted to incorporate a minor overfill factor for the purposes of casting and trimming the specimens.

TABLE 2. TECHNICAL PROPERTIES OF THE AGGREGATE AND FLY ASH

Properties	NFA[a]	RCA[b]	Fly Ash
Gradation	Zone 2	-	-
Fineness Modulus	2.935	6.521	-
Oven Dry Specific Gravity	2.69 g/cm^3	2.31 g/cm^3	2.50 g/cm^3
SSD Specific Gravity	2.71 g/cm^3	2.46 g/cm^3	-
Absorption	0.654 %	6.309 %	-
Water content	4.706 %	4.861 %	-

a. Natural Fine Aggregate
b. Recycled Coarse Aggregate

D. Taguchi Mix Design

The Taguchi design presented in Table 3 was utilized to investigate the synergistic effects of polymer matrix (A), resin–hardener ratio (B), coarse-to-fine aggregate ratio (C), and fly ash content (D) on compressive strength and static modulus of elasticity, while maintaining a tolerable total number of experimental RUNs. Each control factors was examined at three levels according to the requirements in Table 3.

TABLE 3. CONTROL FACTORS AND LEVELS

Code	Control Factors	Levels		
		1	*2*	*3*
A	Polymer Matrix[a]	15%	20%	25%
B	Resin–Hardener Ratio	1 : 1	1.5 : 1	2 : 1
C	Coarse-to-Fine Aggregate Ratio	2 : 1	1 : 1	1 : 2
D	Fly Ash Content[b]	15%	30%	50%

a. Based on the total specimen volume
b. Based on the total fine aggregate volume

Table 4 presents the orthogonal array L9 (3^4) was used to assign the factor-level combinations into nine experimental trials.

In the L9 array, each level of every factor is replicated five and is statistically balanced concerning the other factors. This method enabling the independent estimation of the main effects of A–D with a minimum of nine unique mixtures, as opposed to the $3^4 = 81$ combinations necessitated by a full-factorial design. Five nominally similar specimens were produced for each RUN to conduct compressive testing and determine the modulus of elasticity. Following testing, data from each RUN were examined for outliers utilizing a rigorous statistical criterion (interquartile range and ±2 standard deviation checks).

The Taguchi analysis was carried out using both the arithmetic mean and the S/N ratio of the response. For a "larger-is-better" characteristic like compressive strength, the signal-to-noise ratio (η) for a specific trial with n genuine specimens and recorded responses y_1, y_2, …, y_n was calculated as:

$$\eta = -10 \log_{10} \left(\frac{1}{n} \sum_{k-1}^{n} \frac{1}{y_k{}^2} \right) \tag{6}$$

TABLE 4. ORTHOGONAL ARRAY L9 (3^4) FOR EXPERIMENT

RUN	Mix Design	Materials[a] (cm^3)				
		EPR	*EPH*	*RCA*	*Fine Agr.*	*Fly Ash*
1	A1B1C1D1	10.31	10.31	77.92	33.11	5.84
2	A1B2C2D2	12.38	8.25	58.44	40.91	17.53
3	A1B3C3D3	13.75	6.88	38.96	38.96	38.96
4	A2B1C2D3	13.75	13.75	55.00	27.50	27.50
5	A2B2C3D1	16.50	11.00	36.67	62.33	11.00
6	A2B3C1D2	18.33	9.17	73.33	25.67	11.00
7	A3B1C3D2	17.19	17.19	34.38	48.13	20.63
8	A3B2C1D3	20.63	13.75	68.75	17.19	17.19
9	A3B3C2D1	22.92	11.46	51.56	43.83	7.73
Opt.	A3B2C2D2	20.63	13.75	51.56	36.09	15.47

a. Volume fraction calculation with a total target of 137.5 cm^3

Main-effect plots of the mean and S/N ratio were constructed for each factor to identify trends and candidate optimal levels. ANOVA was then performed on the mean and S/N ratios to quantify the percentage contribution of each factor to the variability in compressive strength. The optimal factor combination identified by the Taguchi analysis is ultimately contrasted with the actual test results derived from this optimal factor mixture. This test is employed to assess the robustness of the mix design predicted by the Taguchi method. The optimal mixture combination is named "RUN Opt." with the proportions determined in absolute volume as described in Table 4.

E. Specimen Preparation

For each RUN experiment, the requisite quantities of resin and hardener were initially quantified and subsequently premixed until a homogeneous binder phase was achieved. In a separate container, the oven-dry RCA, sand, and fly ash were dry-mixed to achieve a uniform aggregate–filler blend. The epoxy binder was then gradually introduced into the aggregate/fly-ash mixture and mixed manually until all particles were thoroughly coated and a consistent polymer concrete mixture was achieved. The fresh polymer concrete was placed into steel cube molds with internal dimensions of 50 × 50 × 50 mm in two layers. Each layer was compacted using rodding and gentle external tapping to reduce air entrapment while preventing segregation, in accordance with

 EISSN: 2961-872X ●PISSN: 2961-8924●DOI: 10.56741/IISTR.esl.002091

the standard procedures for polymer concrete outlined in ASTM C579-96 Method B [13].

Subsequent to casting, the moulds were positioned in a vented oven and subjected to heat curing at 75 ± 2 °C for 6 hours, after which the specimens were demolded [22]. The demoulded cubes were thereafter maintained in the laboratory at (25 ± 2) °C under ambient indoor humidity until they reached 7 days of age. This curing technique aligns with standard procedures for epoxy materials to expedite cross-linking and the enhancement of mechanical properties before testing. Fig. 3 shows the physical and visual qualities of the cube-shaped polymer concrete specimens that have been produced.



Fig. 3. Cube Test Specimen 50 × 50 × 50 mm

F. Mechanical Testing

All mechanical tests were conducted at 7 days on 50 × 50 × 50 mm cubic specimens. Compressive loading was performed in a servo-controlled testing machine as shown in Fig. 4. Compressive loading following the general loading procedure and failure criteria of ASTM C579 for polymer concrete [13]. Axial deformations were recorded simultaneously to obtain the complete stress–strain response for each specimen. Each cube was placed centrally between the loading platens, and a cantilever steel plate with a digital dial gauge was mounted to measure the vertical shortening over a gauge length L_0 equal to the specimen height. During loading, the applied load P and the corresponding deformation ΔL were recorded at regular intervals along the ascending branch of the curve.

The static modulus of elasticity was derived as a chord (secant) modulus from the initial, almost linear segment of the stress–strain curve, in accordance with the conceptual definition in ASTM C469/C469M [23], but applied to cube specimens instead of cylinders. Two points on the ascending branch were identified for each cube:

- $(\sigma_1, \varepsilon_1)$, corresponding to a small reference strain ε_1 (of the order of 50 microstrain) to exclude seating effects and initial slack in the measuring frame;
- $(\sigma_2, \varepsilon_2)$, corresponding to a stress σ_2 of approximately 0.40 f_c, still within the quasi-linear range of the curve



Fig. 4. Mechanical Test Setup

The chord modulus E_c was then calculated as:

$$E_c = \frac{\sigma_2 - \sigma_1}{\varepsilon_2 - \varepsilon_1} \quad (7)$$

This approach treats modulus as the slope of the stress–strain curve in the elastic range and is consistent with the way static modulus is defined in ASTM C469/C469M, while recognising that the present tests were conducted on cube specimens in accordance with the loading geometry of ASTM C579. For verification, the values of Ec were compared with the slope obtained from a least-squares linear regression fitted to the stress–strain data between roughly 5–40% of fc; specimens showing anomalous behaviour or inconsistent curves were checked against the raw data and excluded where necessary.

III. Results and Discussion

A total of 45 epoxy polymer concrete cubes were subjected to compressive testing at 7 days, corresponding to the nine Taguchi L9 mixtures with five nominal repeats each trial. The detailed compressive strength results, mean values, and S/N ratios are summarised in Table 5 and Fig. 5. After excluding extreme values by a formal outlier criterion, the effective number of specimens each RUN varied from four to five. The 7-day compressive strengths ranged from roughly 11 to 57 MPa, with an overall mean of 32.64 MPa and a standard deviation of 11.42 MPa across all trials. This strength range is consistent with the behaviour of epoxy polymer concretes reported in the literature [3], [4].

Table 5. Compressive Strength Test Results

RUN	Number of Trials (MPa)					Mean (MPa)	S/N Ratio[a] (dB)
	R_1	R_2	R_3	R_4	R_5		
1	11.14	12.25	10.91	19.44	20.96	14.94	22.510
2	41.69	39.60	18.68[b]	33.41	39.66	38.59	31.636
3	19.84	14.20	22.52	15.08	18.19	17.97	24.713
4	28.95	36.78	39.32	34.01	29.86	33.78	30.395
5	17.56[b]	31.26	32.04	34.37	31.58	32.32	30.170
6	33.98	38.07	25.56[b]	37.68	39.58	37.33	31.399
7	30.85	35.59	32.05	30.05	24.34	30.58	29.501
8	37.13	55.06	41.32	44.19	53.44	46.23	33.005
9	57.20	41.18	47.10	38.03	37.01	44.10	32.568
All Results:					Mean	32.64	29.544
					Standard Deviation	11.41	

[a.] Characteristic: Larger is Better (Compression Strength)
[b.] Outlier data are excluded from the estimate

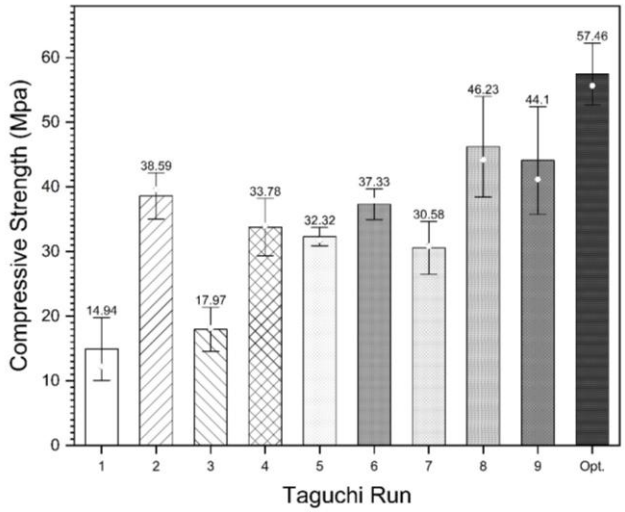

Fig. 5. Compressive Strength Result

A. Taguchi Analysis Based on Compressive Strength

The Taguchi analysis was conducted utilizing both the mean compressive strength and the S/N ratio for the "larger-is-better" characteristic. Fig. 6 summarizes the primary effects of four control factors on mean compressive strength. The average response for each factor at levels 1, 2, and 3 was calculated by aggregating the relevant L9 RUNs. For the mean compressive strength, the main-effect table shows clear trends. Increasing polymer matrix content from 15% (A1) to 20% (A2) and then to 25% (A3) raises the average strength from 23.83 MPa to 34.48 MPa and 40.30 MPa. The resin–hardener ratio also exerts a strong influence: transitioning from 1:1 (B1) to 1.5:1 (B2) increases the mean strength from 26.43 MPa to 39.05 MPa, whereas further increasing to 2:1 (B3) reduces it to 33.13 MPa, indicating an optimum near the stoichiometric or slightly resin-rich condition rather than an excessively high epoxy fraction. The coarse-to-fine aggregate ratio exhibits a similar non-linear pattern, with the 1:1 ratio (C2) giving the highest mean strength, while more coarse-dominant (C1) or fine-dominant (C3) gradations reduce performance. In contrast, the influence of fly ash fraction is more modes. Strength improves somewhat when the Class C fly ash concentration in the fine aggregate climbs from 15% (D1) to 30% (D2) then plateaus or drops marginally at 50% (D3).

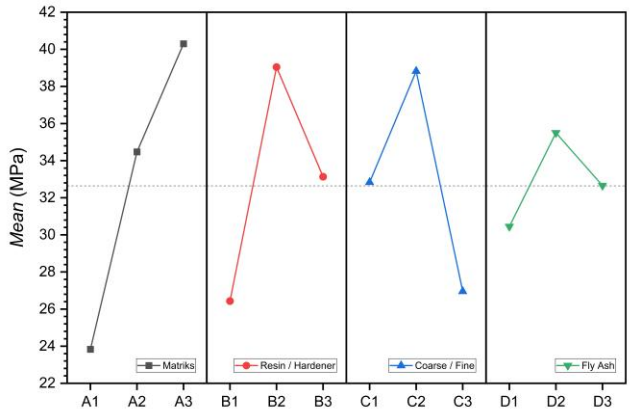

Fig. 6. Main Effects Plot for Means

The main effects plot for S/N ratio resulted from Taguchi method is presented in Fig. 7. The Taguchi analysis utilizing the S/N ratio produces conclusions similar to those derived from the mean analysis, however not identical. For the “larger-is-better” formulation, the S/N ratio rewards mixtures that achieve high strength with low variability. The main-effect table for S/N shows that the optimal levels are again A3 (25% polymer matrix), B2 (1.5:1 resin–hardener ratio), and C2 (1:1 coarse-to-fine ratio), with fly ash exerting a smaller effect. However, the ranges of the S/N responses are compressed compared with those of the means, indicating that some factor combinations with very high average strength also exhibit greater scatter and therefore do not dominate as strongly when robustness is considered.

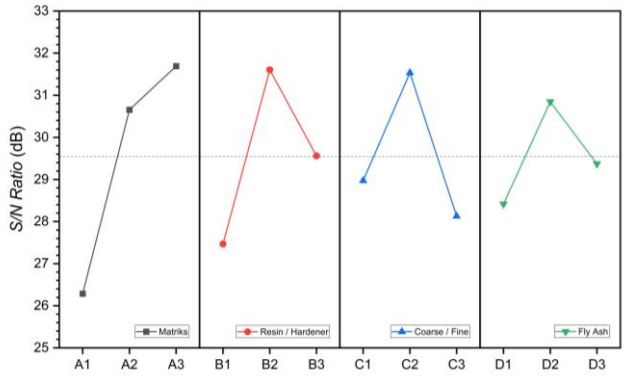

Fig. 7. Main Effects Plot S/N Ratio

The ANOVA of mean compressive strength confirms the relative importance of the factors [Table 6]. Polymer matrix content (A) being the most influential and accounting for approximately 46% of the total variance ($F \approx 10.8$), followed by resin–hardener ratio (B) with about 26% ($F \approx 6.2$) and coarse-to-fine ratio (C) with roughly 23% ($F \approx 5.5$), while fly ash (D) is statistically less significant and therefore pooled into the error. The ANOVA of the S/N ratios leads to a very similar hierarchy [Table 7]. Polymer matrix content (A), resin–hardener ratio (B), and coarse-to-fine aggregate ratio (C) collectively account for approximately 90% of the variance in S/N, with individual contributions of roughly 48%, 25%, and 18%, respectively, while the fly ash factor is aggregated into the error term. The alignment between mean-based and S/N-based analyses reinforces the assertion that the three principal mix parameters govern the behavior of the epoxy polymer concrete. Such concordance between mean and S/N rankings is characteristic of Taguchi methodologies, where the primary sources of variability are directly associated with the control factors rather than extraneous noise.

The dominance of polymer matrix content in this study is consistent with Smoleń *et al.*, who reported that resin volume fraction strongly affects apparent density, porosity, and mechanical performance of polymer concrete [3]. However, the present results also show that increasing polymer content alone is not sufficient to guarantee optimum performance, since the resin–hardener ratio and coarse-to-fine aggregate ratio also contributed substantially to strength variation. This finding supports Ferdous *et al.*, who emphasized that epoxy polymer concrete performance depends on the combined effects of matrix proportion, aggregate distribution, and resin–filler balance [4]. Therefore, the optimum mixture obtained in this study should not be interpreted merely as a high-resin mixture, but as a balanced system in which the polymer matrix, aggregate skeleton, and filler fraction jointly enhance load transfer.

 EISSN: 2961-872X ●PISSN: 2961-8924●DOI: 10.56741/IISTR.esl.002091

TABLE 6. ANOVA TABLE FOR MEAN VALUE

Code	Degree of Freedom	Sum of Square	Variance	F Ratio	Percent
A	2	418.959	418.959	10.77	46.15
B	2	239.414	239.414	6.16	26.37
C	2	211.904	211.904	5.45	23.34
D	(2)	(38.89)	*Pooled*	-	-
Error	2	38.89	19.45	-	4.28
Total	8	907.75			100

TABLE 7. ANOVA TABLE FOR MEAN S/N RATIO VALUE

Code	Degree of Freedom	Sum of Square	Variance	F Ratio	Percent
A	2	49.37	49.372	5.49	47.99
B	2	25.65	25.655	2.85	24.94
C	2	18.86	18.865	2.10	18.34
D	(2)	(8.99)	*Pooled*	-	-
Error	2	8.99	4.49	-	8.74
Total	8	102.88			100

In conclusion, both Taguchi methods indicate that a high polymer matrix content (25%), an intermediate resin–hardener ratio (1.5:1), and a balanced 1:1 coarse-to-fine aggregate ratio are optimal for enhancing compressive strength while maintaining acceptable robustness. The S/N analysis adds nuance by highlighting that some high-strength mixtures can be slightly more sensitive to internal variability, but it does not alter the optimal factor combination.

B. Optimal Mix Design based on Taguchi Method

The primary effect plots and ANOVA of mean compressive strength indicated that the Taguchi analysis consistently recognized the factor combination **A3B2C2D2** as the optimal mix design. Table 8 indicates that the optimal mix design based on ANOVAs has a predicted optimal average compressive strength of 52.891 MPa. This estimate includes a 90% confidence interval of ±11.356 MPa, implying an expected performance range of approximately 41.5–64.2 MPa for the optimal combination. Taguchi analysis and ANOVA based S/N Ratio identifies the optimal factor levels as **A3B2C2** with **D2** designated as the best fly ash level. The predicted optimal mix design with a "larger-is-better" quality characteristic showed a value of 35.740 dB. Assuming a resilient design with minimal variation, this S/N ratio value indicates an anticipated optimal compressive strength of approximately 61.23 MPa. The mean-based and S/N-based Taguchi analyses collectively indicate that the ideal epoxy polymer concrete utilizing RCA should demonstrate 7-day compressive strengths ranging from 53 to 61 MPa.

TABLE 8. ESTIMATE OF OPTIMUM CONDITION OF DESIGN

Code / Level	Level	Contribution		
		Mean	*S/N Ratio*	
A / 3	25%	7.66 MPa	2.14 dB	-
B / 2	1.5 : 1	6.40 MPa	2.06 dB	-
C / 2	1 : 1	6.18 MPa	1.99 dB	-
D / 2	30%	*Pooled*	*Pooled*	-
All Factor		20.25 MPa	6.19 dB	-
Grand Average		32.64 MPa	29.54 dB	-
Expected Result		52.89 MPa	35.74 dB	61.23 MPa
Confidence Interval		± 11.35 MPa	± 5.46 dB	-

Independent testing outcomes of the optimal factor combination via Taguchi analysis produced an average compressive strength of 57.46 MPa, accompanied by a standard deviation of 4.79 MPa. Table 9 shows the experimental mean lies above the mean-based Taguchi prediction but within the 90% confidence interval and moderately below the S/N Ratio-based taguchi. This agreement indicates that the Taguchi framework not only correctly ranked the relative influence of factors but also provided a quantitatively reliable estimate of the expected performance gain at the optimal parameter combination.

TABLE 9. COMPARISON BETWEEN TAGUCHI PREDICTIONS AND EXPERIMENTAL CONFIRMATION AT THE OPTIMAL MIX DESIGN

Method	f'_c (MPa)	CI[a] (Mpa)	Deviation
Taguchi Prediction (Mean)	52.89	± 11.35	7.95 %
Taguchi Prediction (S/N Ratio)	61.23	-	6.66 %
Experimental Confirmation	57.46	-	-

[a.] Confidence Interval

The use of 100% RCA is often associated with reduced mechanical performance in conventional cement-based concrete because adhered mortar increases porosity, absorption, and microcracking [8]–[10]. In contrast, the present study shows that RCA-based epoxy polymer concrete can still achieve a confirmation compressive strength of 57.46 MPa when the mix design is optimized. This result is consistent with Kępniak *et al.*, who reported that recycled aggregate can enhance polymer concrete performance when resin and fine particles form a coating layer around porous recycled grains [5]. The difference between conventional RCA concrete and RCA-based polymer concrete indicates that the weakness of RCA can be partially compensated by the strong adhesion, pore-filling capacity, and low permeability of the polymer matrix. Thus, the findings suggest that RCA should not be treated only as a weaker aggregate phase, but as a porous substrate whose performance depends on the quality of resin penetration and interfacial bonding.

Although fly ash was not the most dominant factor in the main-effect analysis, its role should not be underestimated. Fly ash acts primarily as a micro-filler that modifies packing density and the fine matrix surrounding RCA particles. Similar observations were reported by Rochman *et al.* and Fadiel *et al.*, who showed that fly ash can improve polymer-based composites by filling voids and modifying the resin–filler structure [11], [24]. However, excessive fly ash may increase surface area demand and local viscosity, which can reduce workability and increase the probability of entrapped air. Therefore, the optimum fly ash content of 30% in this study reflects a balance between void filling and mixture workability.

C. Factor Interactions and Severity Index

The main-effect analysis shows that the majority of variance in compressive strength and S/N ratio can be attributed to the individual contributions of polymer matrix content (A), resin–hardener ratio (B), and coarse-to-fine aggregate ratio (C). However, the Taguchi interaction analysis provides additional insight into how pairs of factors jointly influence performance. The interaction study employing a Severity Index (SI) from 0 to 100% categorizes the intensity of two-factor interactions as presented in Table 10. Values over around 70% indicate significant interactions, those between 50% and 70% signify moderate interactions, while values below 50% represent weak-to-moderate interactions that do not dominate over the main effects.

TABLE 10. RELATIVE STRENGTH OF PRESENCE OF INTERACTION AND FACTOR LEVELS

#	Interacting Factor Pairs	OA Columns	SI (%)
1	C × D (Coarse/Fine × Fly Ash)	3 × 4	72.93
2	B × D (Resin/Hardener × Fly ash)	2 × 4	66.33
3	B × C (Resin/Hardener × Coarse/Fine)	2 × 3	56.73
4	A × D (Matrix × Fly ash)	1 × 4	43.27
5	A × C (Matrix × Coarse/Fine)	1 × 3	33.67
6	A × B (Matrix × Resin/Hardener)	1 × 2	27.07

The C × D interaction exhibiting the highest SI (≈ 73%) signifies that the influence of the coarse-to-fine aggregate ratio is significantly contingent upon the fly ash dosage, and conversely. This aligns with the function of fly ash as a fine mineral filler that alters the packing density and rheology of the fine aggregate matrix [11], [24]. At fine-rich mixes excessive fly ash can lead to an over-filled matrix with high surface area demand, potentially increasing entrapped air and local viscosity [24]. A balanced coarse-to-fine agregate ratio with an intermediate quantity of fly ash effectively fills intergranular spaces around RCA particles, reducing porosity and enhancing compressive strength [5]. This phenomenon elucidates the positioning of the optimal interaction for C × D on the Taguchi interaction map.

The B × D interaction (≈ 66%) indicates that the resin–hardener ratio's effect on strength is also dependent on the quantity of fly ash. A slightly resin-rich stoichiometry offers an additional low-molecular-weight epoxy that can permeate the porous RCA surface and wet the fine particles [5]. However, this benefit is contingent upon the presence of sufficient fly ash particles to serve as nucleation sites and micro-fillers [24]. The B × C interaction (≈ 57%) further indicates that the optimum resin–hardener ratio depends on the aggregate skeleton. The beneficial effect of slightly resin-rich stoichiometry is more pronounced when the coarse-to-fine agregate ratio is balanced, as an excessively coarse or fine gradation results in stress concentrations and diminished load transfer [25], despite the same binder chemistry. In other terms, accurate stoichiometry alone cannot rectify an uneven aggregate structure.

The remaining interactions (A × D, A × C, A × B) exhibit lower Severity Indices (≈ 27–43%), implying that they are secondary relative to the main effects and the three dominant interaction pairs. From a Taguchi design perspective, these interaction results support two important conclusions. First, the main effects of factor B and C still dominate the response, as indicated by the ANOVA-derived percentage contributions. Second, the strongest interactions all involve C and/or D, suggesting that aggregate packing and fly ash dosage should be tuned jointly in future mix-design extensions. The fact that the Taguchi-derived optimal mix A3B2C2D2 coincides with the optimal combinations identified in the interaction table (e.g. [C2,D2] and [B2,D2]) lends additional confidence that the chosen factor levels reflect a genuine physical synergy.

D. Static Modulus of Elasticity

Fig. 8 shows the average modulus values for each Taguchi RUN. The average static modulus ranges from about 0.58 GPa to nearly 2.95 GPa. The average static modulus for the Taguchi-optimal mixture reached about 2.89 GPa. To illustrate the determination of modulus for individual specimens, Fig. 9 plots the stress–strain curve of a representative cube from the Taguchi-optimal mixture together with the linear fit used to compute modulus of elasticity.

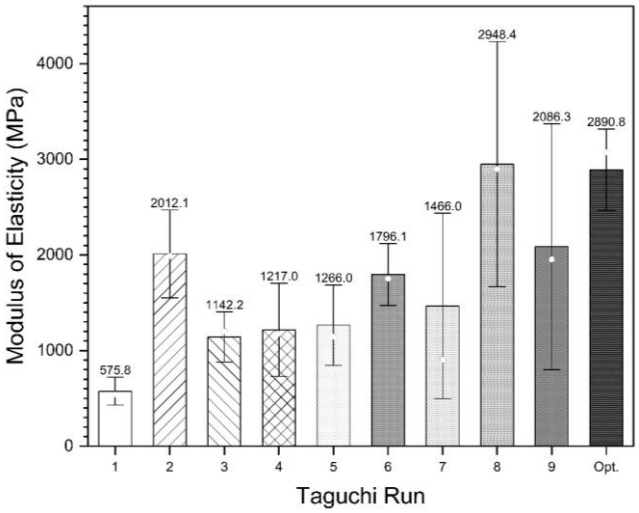

Fig. 8. Modulus of Elasticity Result

The initial segment of the curve demonstrates a nearly linear response up to around 40–45 MPa, with a regression coefficient *R-Square* over 0.998, so validating that the selected strain interval accurately encompasses the elastic zone [23]. Beyond this range, the curve gradually deviates from linearity as microcracks coalesce and the epoxy matrix begins to yield, eventually reaching a peak stress above 55 MPa. The slope of the line that optimally matches the elastic segment of the curve indicates a modulus of around 3.08 GPa for this specific specimen.

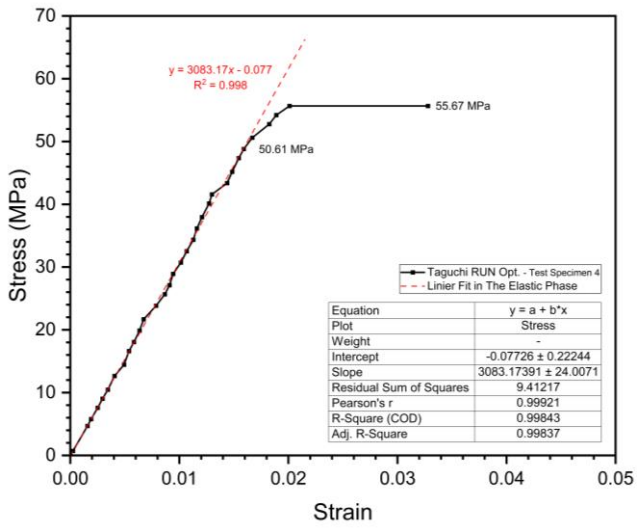

Fig. 9. Stress-Strain Curve and Computation of Elastic Modulus of Polymer Concrete Using Optimal Mixture Specimen

Fig. 10 compares stress–strain curves for selected specimens from each Taguchi RUN. The curves clearly show that mixtures with lower polymer matrix content or sub-optimal aggregate gradation (e.g., RUNs 1 and 3) display a more compliant response, with lower initial slopes and earlier deviation from linearity. Mixtures with resin-rich and well-graded (e.g., RUNs 2, 6, 8, 9, and Opt.) develop steeper elastic branches and higher peak stresses. In several cases the high-resin mixes also exhibit a more gradual post-peak softening, suggesting improved energy absorption capacity and better crack-bridging by the epoxy matrix. These results affirm that

 EISSN: 2961-872X ●PISSN: 2961-8924●DOI: 10.56741/IISTR.esl.002091

the factor combinations deemed best by the Taguchi analysis not only maximize compressive strength but also significantly improve the elastic stiffness of epoxy polymer concrete including 100% recycled coarse material.

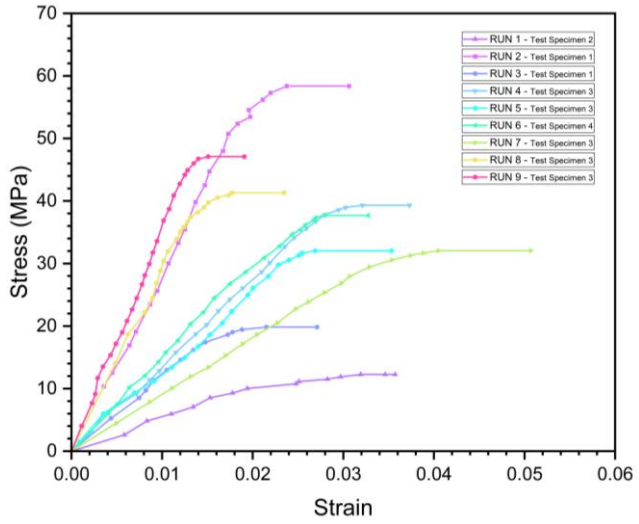

Fig. 10. Stress-Strain Curve of Polymer Concrete Using Taguchi Method Specimen

Fig. 11 shows the relationship between static modulus of elasticity and compressive strength for all valid specimens. A moderate positive correlation is observed (Pearson's r ≈ 0.60), with the regression line:

$$f'_c = 23.53 + 0.00741\,E \tag{8}$$

which can be rearranged to an empirical modulus expression:

$$E = 134.95\,f'_c - 3175 \tag{9}$$

where f_c denotes the compressive strength (MPa) and E represents the static modulus of elasticity (MPa). This trend indicates that mixtures producing stiffer epoxy polymer concrete also tend to exhibit higher compressive strength.

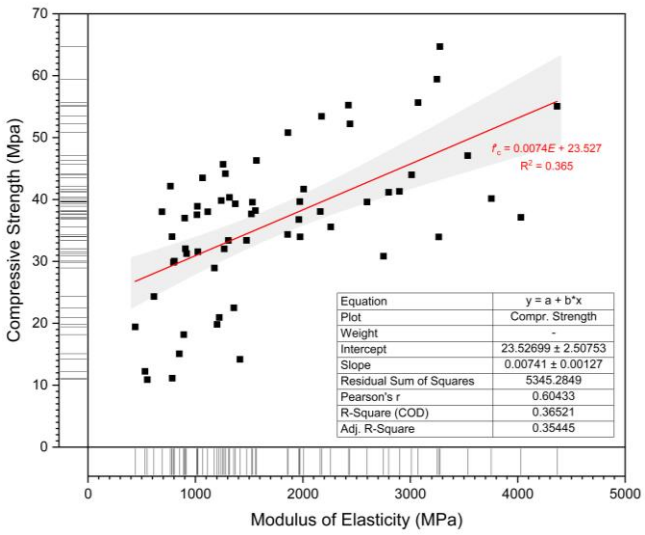

Fig. 11. Relationship Between Compressive Strength and Modulus

However, the coefficient of determination (R-$Square \approx 0.36$) confirms that modulus is controlled not only by strength but also by microstructural features such as resin continuity, aggregate packing, and the volume of internal voids. These observations are consistent with previous studies on polymer and epoxy concretes, which report a positive correlation between E and f_c due to the strong influence of resin volume fraction and aggregate stiffness on elastic response [6], [10].

E. Practical Implications and Future Research Directions

The optimized epoxy polymer concrete developed in this study has practical potential for precast components, repair materials, industrial floors, drainage elements, and chemical-resistant construction products. The confirmation compressive strength of 57.46 MPa indicates that 100% recycled coarse aggregate can be incorporated into epoxy polymer concrete without necessarily compromising mechanical performance when the polymer matrix, aggregate skeleton, and filler content are properly optimized. This finding is relevant for construction sectors facing increasing pressure to reduce natural aggregate consumption and improve the utilization of construction and demolition waste.

From a broader policy perspective, the findings support circular economy-oriented construction strategies by demonstrating that recycled aggregate can be upgraded into higher-value polymer concrete applications rather than being limited to low-grade construction uses. However, further research is required before large-scale implementation. Future studies should include microstructural validation using SEM, X-ray CT, or porosity analysis to confirm resin penetration, void distribution, and interfacial bonding around RCA particles. Long-term durability, cost analysis, life-cycle assessment, and scale-up testing on larger precast elements are also needed to evaluate technical, environmental, and economic feasibility.

IV. Conclusion

This study optimized the mix design and mechanical properties of epoxy polymer concrete incorporating 100% recycled coarse aggregate and Class C fly ash using a Taguchi-based experimental framework combined with an absolute-volume mix design approach. The results demonstrate that the Taguchi method effectively reduced the experimental matrix while still identifying the dominant factors governing compressive strength and stiffness.

The mean response and S/N ratio analyses consistently identified polymer matrix content, resin–hardener ratio, and coarse-to-fine aggregate ratio as the primary factors affecting compressive strength. Fly ash showed a secondary effect as a mineral filler, mainly contributing to void filling and microstructural refinement. The optimum mixture was obtained at 25% polymer matrix content, a resin–hardener ratio of 1.5:1, a balanced coarse-to-fine aggregate ratio of 1:1, and 30% fly ash based on the total fine aggregate volume. This combination produced a predicted compressive strength of 52.89–61.23 MPa, while the independent confirmation test achieved an average compressive strength of 57.46 MPa. The agreement between the predicted and experimental values confirms the reliability of the Taguchi-based optimization approach for epoxy polymer concrete containing recycled aggregate.

The findings also show that the performance of RCA-based epoxy polymer concrete is not controlled by recycled aggregate content alone, but by the combined interaction between polymer matrix proportion, resin–hardener balance, aggregate skeleton, and filler content. The use of 100% RCA did not prevent the material from achieving high compressive strength when the resin system and aggregate packing were

properly optimized. This indicates that the porous and irregular nature of RCA can be partially compensated by resin coating, pore filling, and improved interfacial bonding within the polymer matrix.

The linear relationship between compressive strength and static modulus of elasticity has a positive correlation (Pearson's $r \approx 0.60$). The modulus of elasticity ranged from approximately 0.58 GPa to 2.95 GPa, while the optimized mixture reached about 2.89 GPa. The empirical relationship between compressive strength and modulus suggests that stronger mixtures generally tend to develop stiffer responses, but stiffness is also influenced by resin continuity, aggregate packing, internal voids, and local heterogeneity. Therefore, compressive strength alone is insufficient to fully predict the elastic behavior of epoxy polymer concrete with RCA.

Overall, this study confirms that a Taguchi-based mix design framework can provide a practical and statistically structured basis for developing sustainable epoxy polymer concrete using fully recycled coarse aggregate. The optimized material has potential for precast components, repair materials, industrial floors, drainage elements, and chemical-resistant construction products. Future studies should include microstructural validation using SEM, X-ray CT, or porosity analysis, as well as long-term durability tests, cost assessment, life-cycle assessment, and scale-up evaluation to verify its technical, environmental, and economic feasibility for broader construction applications.

REFERENCES

[1] B. Massoumi Nejad, S. Enferadi, and R. Andrew, "A comprehensive analysis of process-related CO2 emissions from Iran's cement industry," *Clean. Environ. Syst.*, vol. 16, no. January, p. 100251, Mar. 2025, doi: 10.1016/j.cesys.2024.100251.

[2] B. A. Salami *et al.*, "Polymer-enhanced concrete: A comprehensive review of innovations and pathways for resilient and sustainable materials," *Next Mater.*, vol. 4, no. April, p. 100225, Jul. 2024, doi: 10.1016/j.nxmate.2024.100225.

[3] J. Smoleń *et al.*, "The Influence of Resin Volume Fraction on Selected Properties of Polymer Concrete," *Materials (Basel).*, vol. 17, no. 24, p. 6142, Dec. 2024, doi: 10.3390/ma17246142.

[4] W. Ferdous *et al.*, "Optimal design for epoxy polymer concrete based on mechanical properties and durability aspects," *Constr. Build. Mater.*, vol. 232, p. 117229, Jan. 2020, doi: 10.1016/j.conbuildmat.2019.117229.

[5] M. Kępniak, F. Chyliński, P. Łukowski, and P. Woyciechowski, "Recycled Aggregate Integration for Enhanced Performance of Polymer Concrete," *Materials (Basel).*, vol. 17, no. 16, p. 4007, Aug. 2024, doi: 10.3390/ma17164007.

[6] R. Bedi, R. Chandra, and S. P. Singh, "Mechanical Properties of Polymer Concrete," *J. Compos.*, vol. 2013, pp. 1–12, Dec. 2013, doi: 10.1155/2013/948745.

[7] M. R. M. Aliha, D. M. Imani, S. M. Salehi, M. Shojaee, and M. Abedi, "Mixture optimization of epoxy base concrete for achieving highest fracture toughness and fracture energy values using Taguchi method," *Compos. Commun.*, vol. 32, no. March 2021, p. 101150, Jun. 2022, doi: 10.1016/j.coco.2022.101150.

[8] A. Piccinali, A. Diotti, G. Plizzari, and S. Sorlini, "Impact of Recycled Aggregate on the Mechanical and Environmental Properties of Concrete: A Review," *Materials (Basel).*, vol. 15, no. 5, p. 1818, Feb. 2022, doi: 10.3390/ma15051818.

[9] D. Kryeziu, F. Selmani, A. Mujaj, and I. Kondi, "Recycled Concrete Aggregates: A Promising and Sustainable Option for the Construction Industry," *J. Human, Earth, Futur.*, vol. 4, no. 2, pp. 166–180, 2023, doi: 10.28991/HEF-2023-04-02-03.

[10] F. Carrión, L. Montalbán, J. I. Real, and T. Real, "Mechanical and Physical Properties of Polyester Polymer Concrete Using Recycled Aggregates from Concrete Sleepers," *Sci. World J.*, vol. 2014, 2014, doi: 10.1155/2014/526346.

[11] T. Rochman, Sumardi, S. H. Susilo, and H. A. Wardhana, "Vinyl-ester-based polymer concrete incorporating high volume fly ash under tensile, compressive, and flexural loads," *J. King Saud Univ. - Eng. Sci.*, vol. 36, no. 3, pp. 153–163, Apr. 2023, doi: 10.1016/j.jksues.2023.03.001.

[12] ACI Committee 548.1R-09, *Guide for the Use of Polymers in Concrete*. 1997, pp. 1–40.

[13] ASTM Standards C 579 – 96, *Standard Test Methods for Compressive Strength of Chemical-Resistant Mortars, Grouts, Monolithic Surfacings, and Polymer Concretes*, vol. 84, no. July 1996. 2000, pp. 1–6.

[14] R. K. Roy, "A Primer on The Taguchi Method," in *SpringerReference*, Berlin/Heidelberg: Springer-Verlag, 2011. doi: 10.1007/SpringerReference_7290.

[15] G. Taguchi, S. Chowdhury, and Y. Wu, *Taguchi's Quality Engineering Handbook*. Wiley, 2004. doi: 10.1002/9780470258354.

[16] S. H. Park and J. J. Kim, "Quality Engineering Using Robust Design and Analysis," 1997, pp. 3–15. doi: 10.1007/978-3-642-59268-3_1.

[17] E. Teimortashlu, M. Dehestani, and M. Jalal, "Application of Taguchi method for compressive strength optimization of tertiary blended self-compacting mortar," *Constr. Build. Mater.*, vol. 190, pp. 1182–1191, Nov. 2018, doi: 10.1016/j.conbuildmat.2018.09.165.

[18] K. J. Le Lee and S. F. Wong, "Multi-Objective Taguchi Optimization of Cement Concrete Incorporating Recycled Mixed Plastic Fine Aggregate Using Modified Fuller's Equation," *Buildings*, vol. 13, no. 4, p. 893, Mar. 2023, doi: 10.3390/buildings13040893.

[19] H. Mortazavi Bak, M. Noorbakhsh, A. M. Halabian, M. Rowshanzamir, and H. Hashemolhosseini, "Application of the Taguchi Method to Enhance Bearing Capacity in Geotechnical Engineering: Case Studies," *Int. J. Geomech.*, vol. 21, no. 9, pp. 1–14, Sep. 2021, doi: 10.1061/(ASCE)GM.1943-5622.0002133.

[20] F. S. Ackah, W. Hailiang, F. Huaiping, L. Cheng, and L. Z. Feng, "Use of Taguchi method to evaluate the unconfined compressive strength of quicklime stabilized silty clayey subgrade," *Case Stud. Constr. Mater.*, vol. 17, no. August, p. e01417, Dec. 2022, doi: 10.1016/j.cscm.2022.e01417.

[21] P. Suraneni, L. Burris, C. R. Shearer, and R. D. Hooton, "ASTM C618 Fly Ash Specification: Comparison with Other Specifications, Shortcomings, and Solutions," *ACI Mater. J.*, vol. 118, no. 1, pp. 157–167, Jan. 2021, doi: 10.14359/51725994.

[22] D. Lascano, L. Quiles-Carrillo, S. Torres-Giner, T. Boronat, and N. Montanes, "Optimization of the Curing and Post-Curing Conditions for the Manufacturing of Partially Bio-Based Epoxy Resins with Improved Toughness," *Polymers (Basel).*, vol. 11, no. 8, p. 1354, Aug. 2019, doi: 10.3390/polym11081354.

[23] ASTM Standards C 469/C 469M − 14, *Standard Test Method for Static Modulus of Elasticity and Poissons Ratio of Concrete in Compression*, 2008th ed. West Conshohocken, PA: ASTM International, 2014, pp. 1–5. doi: 10.1520/C0469.

[24] A. A. M. Fadiel, N. S. Mohammed, A. B. A. Rahman, E. A. B. Ali, T. Abu-Lebdeh, and F. I. T. Petrescu, "Effect of Fly Ash on Mechanical Properties of Polymer Resin Grout," *Biomimetics*, vol. 8, no. 5, 2023, doi: 10.3390/biomimetics8050392.

[25] P. Cao, G. Liang, X. Chai, Q. Liu, and M. Lv, "Effects of Aggregate Gradation, Content, and Size Range on the Mechanical and Damping Properties of Polymer Concrete for Precision Machine Tool Beds," no. 1158. pp. 1–16, 2025. doi: 10.2139/ssrn.5084432.

 EISSN: 2961-872X ●PISSN: 2961-8924●DOI: 10.56741/IISTR.esl.002091